Journal of Power Sources, 2 (1977/78) 137 - 146

EXPANDER ACTION AT THE Pb(Hg)/$PbCl_2$ INTERFACE

R. G. BARRADAS, S. FLETCHER and J. D. PORTER
Department of Chemistry, Carleton University, Ottawa, Ontario K1S 5B6 (Canada)
(Received December 21, 1976)

Summary

The influence of ammonium lignosulphonate on the kinetics of formation of thick films of $PbCl_2$ is described. It is shown that geometric factors need to be considered as well as the influence of the additive on the rates of lattice growth (k_1, k_2) and the nucleation rate constant (A). The results indicate that expanders may be of use in sea-water activated batteries.

Introduction

For many years expanders (usually derivatives of lignosulphonic acid) have been added to the negative plates of lead–sulphuric acid batteries. The well-known results of this process are to create a better high discharge rate at low temperatures, and also to effect improvements in the cycle life of the battery. Early experimental data have been reviewed in detail by Ritchie [1] and Willihnganz [2]. Unfortunately, however, there appears to be no clear consensus as to the mode of action of expander materials. As a result of this, there has been an increase in theoretical interest in this field in recent years [3 - 17]. In the present communication, we investigate the influence of ammonium lignosulphonate on the formation of thick films of lead chloride on lead amalgam electrodes. This is of interest because of the application of $Pb/PbCl_2$ systems to sea-water activated batteries [18 - 21]. It is shown that, as well as inhibiting the nucleation and growth of the lead chloride multilayer, the ammonium lignosulphonate also changes the morphology of the resultant deposit. This change of morphology is amenable to mathematical interpretation under potentiostatic conditions.

The fundamental kinetics of the $Pb/PbCl_2$ system have been considered previously [20, 21]. This knowledge provided a sound basis for the investigation of the effects of ammonium lignosulphonate on the electrocrystallization process. A particularly advantageous aspect of this work is that highly reproducible, fresh amalgam surfaces could be generated for each individual measurement, in contrast to the more usual solid electrode systems. A natural consequence of this is that the influence of expander material on the rate constants for lattice growth could be clearly and reproducibly determined.

A further advantage of amalgam electrodes over solid electrodes is the complete absence of intergrain boundaries, surface defects, inclusions, oxide films etc., the presence of which normally complicate the interpretation of experimental data. The irreproducible nature of these surface features on solid electrodes is one of the major reasons for our present lack of clear understanding regarding the action of expander materials on the formation and reduction of anodic films.

Experimental

The experimental details have been described elsewhere [20]. The ammonium lignosulphonate was a commercial product (Lignosol C-16, Lignosol Chemicals Ltd, Québec). A typical analysis of the product is given in Table 1.

TABLE 1

H_2O	5 %
Ash	1.7%
Total sulphur	7.5%
Organic sulphur	7.3%
Calcium	< 0.1%
Sodium	traces
Organic nitrogen	1.4%
Nitrogen (ammonia)	1.8%
Methoxyl	8.2%
Impurities (Mg, Fe, Mn, Zn, Cu, heavy metals)	traces
Equivalent weight	> 320

Results

Figure 1 shows linear potential sweep voltammograms under conditions of continuous cycling, showing the influence of the addition of 0.73 g/l Lignosol C-16. The electrode consists of a 1.68% lead amalgam, whilst the electrolyte is 1.0 *M* HCl. In the absence of Lignosol C-16 normal behaviour is exhibited, namely the dissolution of Pb^{2+} ions as $PbCl_n^{2-n}$ complexes followed by (A) monolayer formation and (B) multilayer formation [20]. The formation of the multilayer results in the passivation of the electrode surface at ~ −400 mV *vs.* S.C.E. Upon reversing the linear potential scan, the surface species are reduced in one unresolved peak at ~ − 520 mV. The influence of the addition of Lignosol C-16 is clear; the fine structure of the voltammogram disappears and approximately three times as much charge is required to passivate the electrode surface. On reverse scan, the reduction of the surface $PbCl_2$ species is severely inhibited. A long "tail" is seen to exist

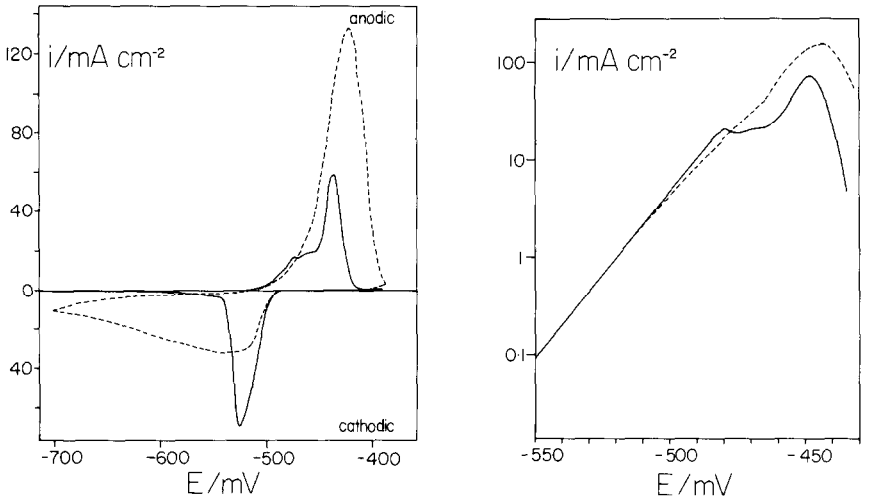

Fig. 1. Continuous-cycle linear potential sweep voltammograms for the 1.68% Pb(Hg)/$PbCl_2$ system (1 *M* HCl, ν = 50 mV/s) recorded in the absence (——) and presence (----) of Lignosol C-16 (0.73 g/l).

Fig. 2. Single-shot linear potential sweep voltammograms for the 1.68% Pb(Hg)/$PbCl_2$ system (1 *M* HCl, ν = 50 mV/s) recorded in the absence (——) and presence (----) of Lignosol C-16 (0.97 g/l).

between − 500 and − 700 mV, suggesting that the formation of the $PbCl_2$ deposit on forward scan occurs at some distance away from the electrode surface, such that Pb^{2+} species have to diffuse back towards the electrode surface. Some reduction of Pb^{2+} species, however, also occurs in the solid state region (− 520 mV) so that this evidence is not entirely unambiguous.

The effect of Lignosol C-16 on the anodic dissolution of Pb^{2+} species is shown in Fig. 2. It is clear that both with and without the additive a Tafel slope of 30 mV/decade is observed. This corresponds to the familiar Nernstian reaction:

$$Pb(Hg) \overset{-2e}{\rightleftharpoons} Pb^{2+} \rightleftharpoons PbCl^{+} \rightleftharpoons PbCl_{2(soln)} \rightleftharpoons PbCl_3^{-} \rightleftharpoons PbCl_4^{2-} \quad \text{etc.} \qquad (1)$$

as observed previously [20]. At high anodic overpotentials, some differences become apparent. In particular, monolayer formation appears to be largely inhibited (− 480 mV) whilst the dissolution reaction continues unabated. Finally (− 460 mV) the solid state initiation of a thick $PbCl_2$ deposit begins, after which the electrode rapidly passivates.

Figure 3 shows successive cyclic voltammograms on a fresh amalgam drop after injection of a large quantity (4.89 g/l) of Lignosol C-16. The solution was 0.67 *M* in HCl *i.e.* at the solubility minimum of $PbCl_2$ complexes [22 - 25]. With increasing time an increasing amount of charge is required to passivate the electrode; this gradual progression is probably

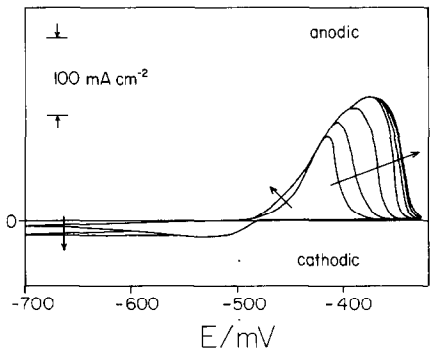

Fig. 3. Successive continuous-cycle linear potential sweep voltammograms recorded on a fresh amalgam drop (1.68% Pb(Hg), 0.67 *M* HCl, ν = 50 mV/s) in the presence of Lignosol C-16 (4.89 g/l).

associated with the non-equilibrium adsorption of ammonium lignosulphonate as thick multilayers during the time-scale of the experiment [3]. Note also that the cathodic reaction is inhibited almost entirely. Because of the low ionic strength of solution used here, and also the high current densities observed, there is necessarily a large contribution in the voltammograms from ohmic overpotential. Nevertheless, the effects are clear and reproducible.

As shown in a previous communication [20] the kinetics of the nucleation and growth of a thick layer of $PbCl_2$ on the amalgam surface may be investigated by the potential step technique. In the absence of Lignosol C-16, the transients correspond to the mechanism of Armstrong *et al.* [22]. This is shown in Fig. 4 where the current response of the system is illustrated for a sequence of nucleation overpotentials. Analysis of the transients is performed in terms of the variables:

$$i_m = \frac{nFk_2}{4} \tag{2}$$

$$t_m = \left(\frac{3\rho^2 \ln 2}{\pi M^2 k_1^2 A} \right)^{1/3} \tag{3}$$

where k_2 is the rate constant describing crystal growth perpendicular to the electrode surface, k_1 is the rate constant parallel to the electrode surface, and A is the nucleation rate constant.

In the presence of Lignosol C-16 certain profound changes become evident in the current–time curves (Fig. 5). The charge required to passivate the electrode surface increases three-fold, and at the same time the shape of the response becomes broader. This is further exemplified in Fig. 6, where the experimental data are shown plotted in non-dimensional form. It is also apparent, by comparison of Figs. 4 and 5, that shifts also occur in the potential scale which are not detected in the non-dimensional analysis.

Typical potential shifts are shown in terms of $\log(i_m)$ and $\log(t_m)$ in Figs. 7(a) and 7(b). Some curvature is apparent in both instances due to the

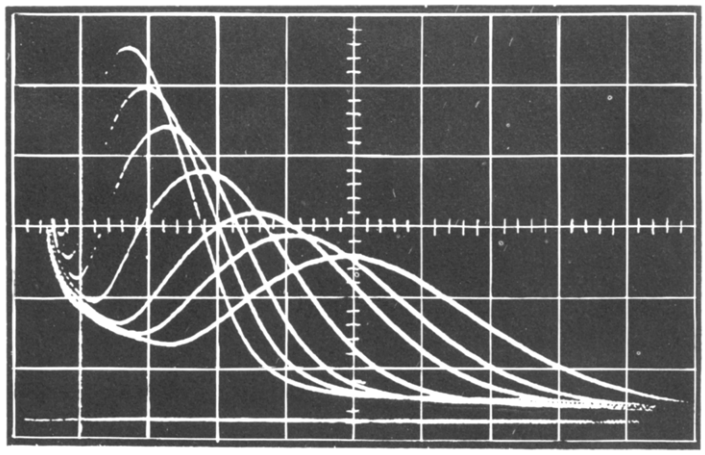

Fig. 4. Representative potentiostatic transients for the 1.68% Pb(Hg)/$PbCl_2$ system in the absence of Lignosol C-16 (1 *M* HCl, A = 0.073 cm^2). E = — 444, — 442, — 440, — 436, — 432, — 428, — 424 mV respectively. Horiz. = 20 ms/cm, vert. = 5 mA/cm.

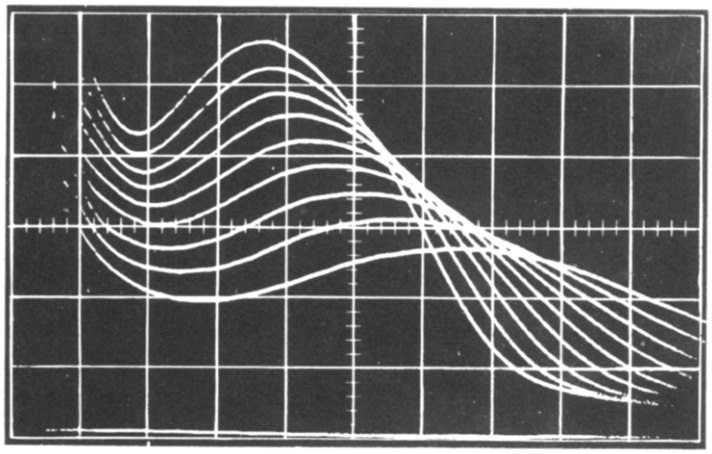

Fig. 5. Representative potentiostatic transients for the 1.68% Pb(Hg)/$PbCl_2$ system (1 *M* HCl, A = 0.073 cm^2) in the presence of a small amount of Lignosol C-16 (1.15 mg/l). E = — 435, — 430, — 425, — 420, — 415, — 410, — 405, — 400, — 395 mV. Horiz. = 10 ms/cm, vert. = 5 mA/cm.

presence of uncompensated ohmic overpotential. In general, though, it can be seen that the curves are shifted to more anodic overpotentials with increasing concentration of Lignosol C-16. An exception to this, however, occurs when small concentrations of Lignosol C-16 are initially added to the cell. Under these circumstances the curves are shifted somewhat to more cathodic overpotentials.

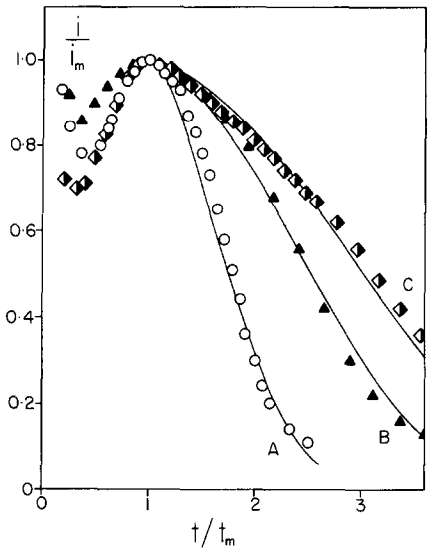

Fig. 6. Potentiostatic transients plotted in non-dimensional form for the 1.68% Pb(Hg)/$PbCl_2$ system, illustrating the influence of Lignosol C-16. Included in each case is the best fit transient computed according to eqn. (5). A, 1 *M* HCl, 1.15 mg/l lignosol, $E = -395$ mV, $x = 0.06$. B, 3 *M* HCl, 38.5 mg/l lignosol, $E = -503$ mV, $x = 0.01$. C, 1 *M* HCl, 97.4 mg/l lignosol, $E = -455$ mV, $x = 0.005$.

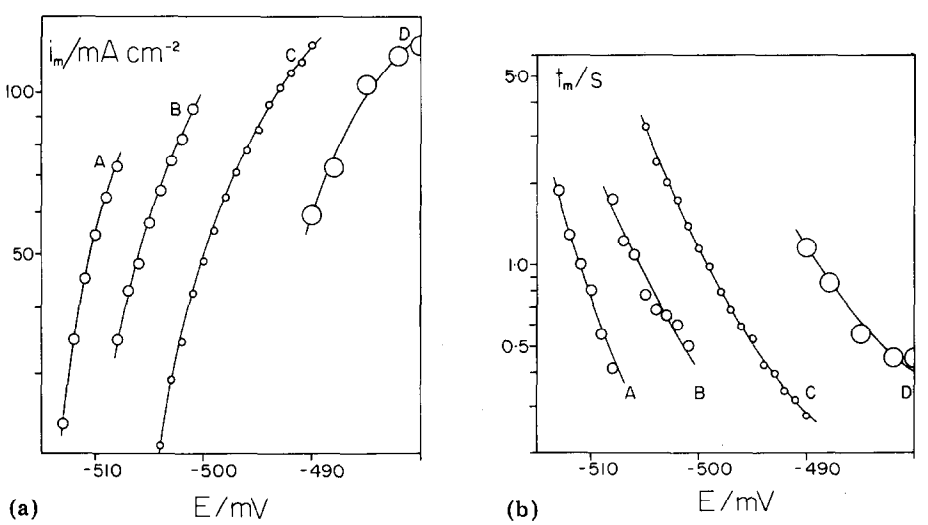

Fig. 7(a). i_m data from potentiostatic transients as a function of E for the 2.35% Pb(Hg)/$PbCl_2$ system (3 *M* HCl). Lignosol C-16 concentrations: A, 1.93 mg/l; B, 38.5 mg/l; C, 0 mg/l; D, 177 mg/l.

Fig. 7(b). t_m data from potentiostatic transients as a function of E for the 2.35% Pb(Hg)/$PbCl_2$ system (3 *M* HCl). Lignosol C-16 concentrations: A, 1.93 mg/l; B, 38.5 mg/l; C, 0 mg/l; D, 177 mg/l.

Discussion

In a previous communication [21] we considered the equation describing the behaviour of the current due to the nucleation and growth of a three-dimensional deposit following the application of a potential step to an electrode, in order to describe the active–passive transition of the $Pb/PbCl_2$ interface. The model chosen was that of Armstrong *et al.* [22]. At short times in the experimental transient, the current is given by:

$$i(t) = f(k_1, k_2, A) = nFk_2 \left[1 - \exp\left(\frac{-\pi M^2 k_1^2 A t^3}{3\rho^2}\right)\right] \tag{4}$$

When the growth of the deposit leads to passivation, this solution becomes more complex, because it becomes necessary to describe the time-dependence of the diffusion of species from the uncovered area of the electrode to the growth sites. This may be achieved, to a first approximation, by definition of a non-zero time-independent constant (x) which relates the rate of growth of the deposit to the decreasing area of the substrate. The overall result is [21]:

$$i(t) = f(k_1, k_2, A, x) = nFk_2 \left[1 - \exp\left(\frac{-\pi M^2 k_1^2 A t^3}{3\rho^2}\right)\right] \left[\exp\left(\frac{-\pi M^2 k_1^2 A t^3}{3\rho^2}\right)\right]^x \tag{5}$$

This function is illustrated in Fig. 8 for an arbitrary potential, where:

$$i_m = \frac{x^x}{(1+x)^{1+x}} \cdot nFk_2 \tag{6}$$

and

$$t_m = \left[\frac{3\rho^2 \cdot \ln\left(\frac{1+x}{x}\right)}{\pi M^2 k_1^2 A}\right]^{1/3} \tag{7}$$

Equation (5) may be used in semi-empirical fashion to describe the influence of Lignosol C-16 on the experimental transients. This implies a model of expander action in which k_2 is diminished in the presence of the expander material, but not as much as k_1. The model is a geometrical one, and therefore does not depend on the mode of action of the expander. However, it may be surmised that expanders generally influence passivation via their strong adsorption at the metal–electrolyte interface, as well as their direct adsorption on the surface of the growing crystal. Under extreme conditions, therefore, crystal growth would be expected to be dendritic. However, under intermediate conditions the present model should suffice.

Theory and practice are compared in Fig. 6, where the experimental data of Fig. 5 are plotted superimposed upon the non-dimensional form of eqn. (5). Note that the theoretical transients correspond to experimental data at various values of x. Such an analysis indicates a fairly consistent, though not linear, interrelationship between expander concentration and x. However, besides this geometrical effect it is clear from Fig. 7(a) that the

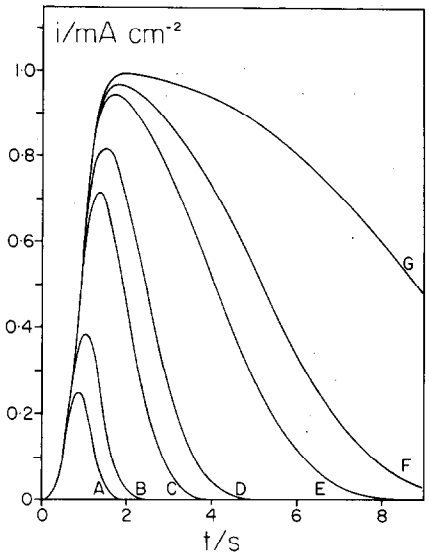

Fig. 8. Variation of the parameter x, according to eqn (5). x = (A) 1.0 (B) 0.5 (C) 0.1 (D) 0.05 (E) 0.01 (F) 0.005 (G) 0.001. The scales are arbitrary.

absolute magnitude of k_2 is, in general, diminished with increasing concentration of additive.

A similar trend is observed in t_m data. Unfortunately, rigorous analysis is not possible because of the inseparability of k_1 and A in eqn. (7). It is quite likely that both terms are affected in complex fashion by the addition of expander material.

Conclusion

The effect of the expander material Lignosol C-16 on the formation of the thick layer of $PbCl_2$ at the Pb(Hg)/HCl interface is complex. It is necessary to consider geometric factors as well as the influence of the additive on the rates of lattice growth (k_1, k_2) and the nucleation rate constant (A). The increase in charge required to passivate the electrode surface is ascribed to geometrical factors in the emergent deposit. Because of the relative enhancement of k_2 compared to k_1, the passivating layer develops at greater distances from the electrode surface, and this contributes to the inhibition of the reverse reaction. This inhibition is probably also related to the adsorption of the Lignosol C-16 at the metal–solution interface [3].

At high Lignosol C-16 concentrations the experimental data indicate that the rate constants for lattice growth are diminished. This allows the dissolution of Pb^{2+} ions (in the form of soluble $PbCl_n^{2-n}$ complexes) to occur quite freely into solution. This is not only clear from the voltammograms, but may also be seen at short times in the experimental transients.

It therefore appears that expander materials influence $PbCl_2$ formation in a similar manner to $PbSO_4$ formation; hence they may be expected to exert similar beneficial effects in the corresponding battery system.

Symbols used in text

E Potential
t Time
ν Scan rate
k_1 Rate constant describing crystal growth parallel to the electrode surface
k_2 Rate constant describing crystal growth perpendicular to the electrode surface
A Nucleation rate constant
M Molecular weight
ρ Density of deposit
x A time-independent constant
i_m Current maximum in growth transient
t_m Time to current maximum in growth transient

Acknowledgements

This work has been supported by a grant from the National Research Council of Canada.

Lignosol C-16 was kindly supplied by Reed Pulp and Paper Group, Québec.

References

1 E. J. Ritchie, Trans. Electrochem. Soc., 92 (1947) 229.
2 E. Willihnganz, Trans. Electrochem. Soc., 92 (1947) 281.
3 M. P. J. Brennan and N. A. Hampson, J. Electroanalyt. Chem. Interfacial Electrochem., 48 (1973) 465.
4 M. P. J. Brennan and N. A. Hampson, J. Electroanalyt. Chem. Interfacial Electrochem., 52 (1974) 1.
5 M. P. J. Brennan and N. A. Hampson, J. Electroanalyt. Chem. Interfacial Electrochem., 54 (1974) 263.
6 G. Archdale and J. A. Harrison, J. Electroanalyt. Chem. Interfacial Electrochem., 34 (1972) 21.
7 G. Archdale and J. A. Harrison, J. Electroanalyt. Chem. Interfacial Electrochem., 39 (1972) 357.
8 G. Archdale and J. A. Harrison, J. Electroanalyt. Chem. Interfacial Electrochem., 43 (1973) 321.
9 E. G. Yampol'Skaya and B. N. Kabanov, J. Appl. Chem. U.S.S.R., 37 (1964) 2501.
10 E. G. Yampol'Skaya, M. I. Ershova, V. V. Surikov, I. I. Astakhov and B. N. Kabanov, Soviet Electrochem., 8 (1972) 1209.
11 E. G. Yampol'Skaya, I. A. Smirnova, I. Ershova, S. A. Saponitskii and L. I. Kryukova, Soviet Electrochem., 8 (1972) 1289.

12 T. F. Sharpe, J. Electrochem. Soc., 116 (1969) 1639.
13 T. F. Sharpe, Electrochim. Acta, 14 (1969) 635.
14 I. N. Maksimova and N. V. Fedotov, Zh. Prikl. Khim. (Leningrad) 44 (12) (1971) 2753.
15 Sekido, Satoshi, Ichimura and Hideyuki, Denki Kagaku Oyobi Kogyo Butsuri Kagaku, 37 (1969) 168.
16 A. Hayashi and Y. Namura, Kami-pa Gikyoshi, 21 (1967) 393.
17 I. A. Aguf, M. A. Dasoyan, L. A. Ivanenko, E. V. Parshikova, K. M. Solov'Eva, Sb. Rab. Khim. Istochrikan, Toka. Nauch. Issled. Akkumulyatorn. Inst., 5 (1970) 21.
18 A. A. Vyselkov and G. Rogova, Chem. Abstr. 52 (1958) 10770, (U.S.S.R. Pat. 109,345).
19 J. R. Coleman, J. Appl. Electrochem., 1 (1971) 65.
20 R. G. Barradas, S. Fletcher and J. D. Porter, J. Electroanalyt. Chem. Interfacial Electrochem., 80 (1977) 295.
21 R. G. Barradas, F. C. Benson and S. Fletcher, J. Electroanalyt. Chem. Interfacial Electrochem., 80 (1977) 305.
22 R. D. Armstrong, M. Fleischmann and H. R. Thirsk, J. Electroanalyt. Chem., 11 (1966) 208.
23 G. P. Haight, Jr. and J. R. Peterson, Inorg. Chem., 4 (1965) 1073.
24 F. Vierling, G. Scarsch and J. Bye, Rev. Chim. Miner., 3 (1966) 875.
25 F. Vierling, Bull. Soc. Chim. France, 22 (1971) 25.